U2AF-homology motif interactions are required for alternative splicing regulation by SPF45

Lorenzo Corsini^{1,6}, Sophie Bonnal^{2,6}, Jerome Basquin¹, Michael Hothorn¹, Klaus Scheffzek¹, Juan Valcárcel² & Michael Sattler^{1,3–5}

The U2AF-homology motif (UHM) mediates protein-protein interactions between factors involved in constitutive RNA splicing. Here we report that the splicing factor SPF45 regulates alternative splicing of the apoptosis regulatory gene FAS (also called CD95). The SPF45 UHM is necessary for this activity and binds UHM-ligand motifs (ULMs) present in the 3' splice site—recognizing factors U2AF65, SF1 and SF3b155. We describe a 2.1-Å crystal structure of SPF45-UHM in complex with a ULM peptide from SF3b155. Features distinct from those of previously described UHM-ULM structures allowed the design of mutations in the SPF45 UHM that selectively impair binding to individual ULMs. Splicing assays using the ULM-selective SPF45 variants demonstrate that individual UHM-ULM interactions are required for FAS splicing regulation by SPF45 *in vivo*. Our data suggest that networks of UHM-ULM interactions are involved in regulating alternative splicing.

In eukaryotic organisms, the outcome of the splicing reaction can be changed by activating alternative splice sites or by selectively skipping or including exons¹. For example, the *Drosophila melanogaster* protein Sex lethal (Sxl), exclusively present in female flies, influences alternative splicing of exon 3 in its own precursor messenger RNA (premRNA) by a positive feedback loop². *In vitro* experiments have shown that binding of Sxl to the splicing factor SPF45 is required to inhibit the ligation of exon 3 (ref. 3) and to promote the production of the functional form of Sxl. However, it is not known how SPF45 can link Sxl to the splicing machinery and mediate its function in splicing regulation.

SPF45 consists of an N-terminal region that is predicted to be unstructured, followed by a G-patch motif⁴ and a C-terminal RNA recognition motif (RRM). The \sim 40-residue G-patch motif, predicted to adopt an α -helical conformation, has seven highly conserved glycines and has been shown to form protein-protein⁵ and protein–nucleic acid^{6,7} interactions. The C-terminal RRM domain binds U2A' and is necessary for *Sxl* splicing regulation by SPF45 in *Drosophila*⁸. The C-terminal RRM domain is homologous to protein-binding RRMs found in the large (U2AF65) and small (U2AF35) subunits of the U2 auxiliary factor (U2AF) heterodimer. RRMs with similar sequence features as in U2AF are also found in many other nuclear proteins, such as PUF60, KIS kinase, SPF45 and HCC1, and were thus named U2AF-homology motifs⁹ (**Fig. 1a**).

In contrast to canonical RRM domains¹⁰, UHMs have degenerate RNP1 and RNP2 motifs and contain an additional Arg-Xaa-Phe amino acid sequence^{9,11,12}. UHMs of U2AF have been shown to

bind tryptophan-containing linear peptide motifs^{11,12}, which we call UHM-ligand motifs. Atomic-detail structures have been determined for the UHMs of the constitutive splicing factors U2AF65 and U2AF35 bound to ULMs in the N-terminal regions of splicing factor-1 (SF1) and U2AF65, respectively^{11,12}. The two complexes share similar modes of molecular recognition of the ligand peptides. The ligand tryptophan is bound in a hydrophobic pocket, while basic and acidic ligand residues flanking the tryptophan (**Fig. 1b**) mediate electrostatic interactions with the UHM. The conservation of these molecular interfaces suggests that a similar UHM-ULM recognition mode is also shared by other UHM proteins, including SPF45.

In higher eukaryotes, U2AF35-UHM interacts with the ULM in the N terminus of U2AF65 to form a stable U2AF heterodimer. The U2AF heterodimer and the interaction of U2AF65-UHM with the SF1 ULM contribute to the cooperative binding of these splicing factors to RNA sequences at the 3' splice site during spliceosome assembly: in complex E, SF1, U2AF65 and U2AF35 bind the branchpoint sequence, the polypyrimidine tract and the AG dinucleotide of the 3' splice site, respectively. The UHM-ULM interactions between these splicing factors enhance the binding affinity to the intron RNA^{13–15}. After ATP-dependent structural rearrangements of the nascent spliceosome, SF1 is replaced by the 155 kDa-subunit of splicing factor-3b (SF3b155) in complex A^{16,17} (Fig. 1c). SF3b155 contains five predicted ULMs and has been shown to bind U2AF65-UHM *in vitro*^{18,19}.

The role of UHM domains in other proteins (**Fig. 1a**) that have been linked to constitutive or alternative pre-mRNA splicing^{3,20–23} is less well understood. The presence of a UHM in these proteins

Received 2 January; accepted 3 May; published online 24 June 2007; corrected after print 2 July 2007; doi:10.1038/nsmb1260

¹European Molecular Biology Laboratory (EMBL), Meyerhofstr. 1, D-69117 Heidelberg, Germany. ²Centre de Regulació Genòmica, Dr. Aiguader 88, 08003 Barcelona, Spain. ³GSF-National Research Center for Environment and Health, Ingolstädter Landstr. 1, 85764 Neuherberg, Germany. ⁴Munich Center for Integrated Protein Science and ⁵Department Chemie, Technische Universität München, Lichtenbergstr. 4, 85747 Garching, Germany. ⁶These authors contributed equally to this work. Correspondence should be addressed to M.S. (sattler@embl.de).

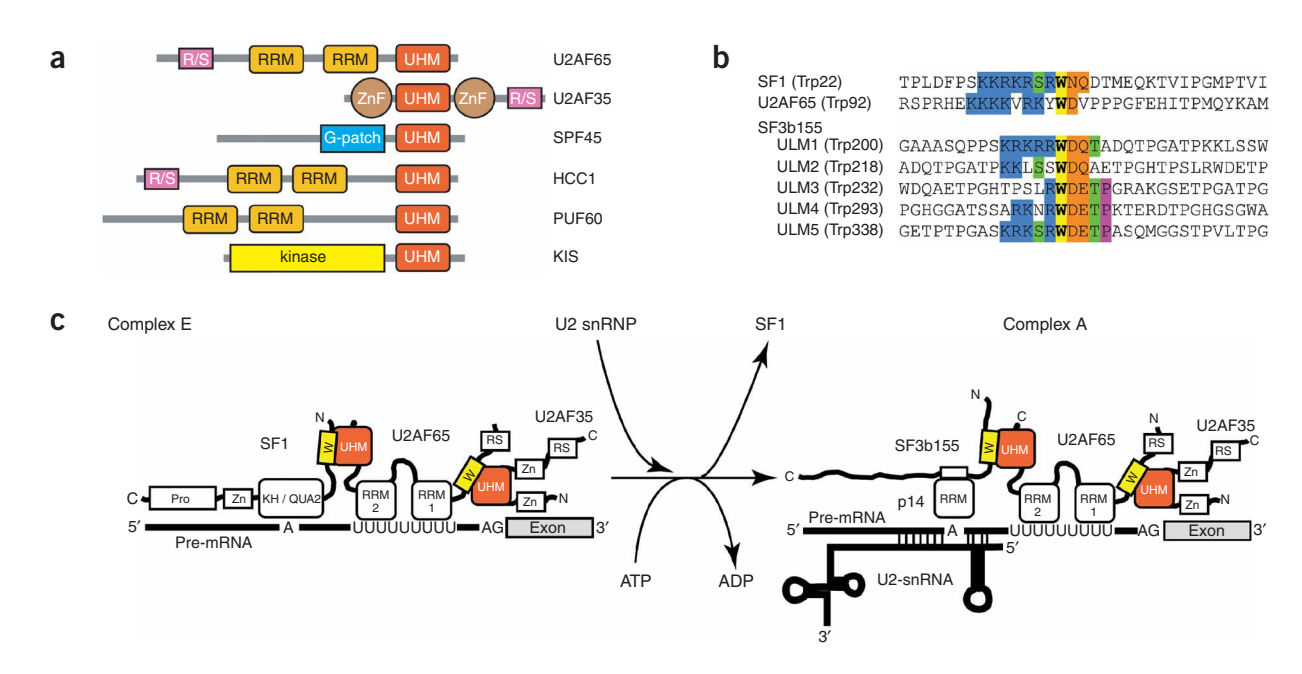


Figure 1 U2AF homology motifs and ligands in splicing factors. (a) Domain alignment of proteins that contain a UHM. (b) Alignment of ULM sequences in U2AF65, SF1 and SF3b155. Conserved residues are colored as follows: blue, basic residues preceding conserved tryptophan; yellow, conserved tryptophan; orange, acidic and Asn/Gln-type residues following tryptophan; green, conserved and potentially phosphorylated serine and threonine residues; purple, proline adjacent to threonine. (c) Schematic drawing of 3' splice sites in spliceosomal complexes E and A.

suggests that they may bind ULMs in splicing factors—for example, those of SF1, U2AF65 and possibly SF3b155. However, it is not known whether and how these UHMs, including the SPF45 UHM, contribute to the regulation of alternative splicing.

Among the huge number of transcripts that can be differentially spliced in humans is FAS (also called CD95 or APO-1). It can be spliced to encode a proapoptotic, single-pass transmembrane form, also known as the 'death receptor', or to encode a soluble, antiapoptotic form that lacks the transmembrane domain encoded on exon 6 (ref. 24). The transmembrane-receptor isoform of FAS triggers the apoptosis program when it binds FAS ligand (FASL) and activates caspase cascades²⁵. Exon 6 skipping results in expression of the soluble isoform of FAS, which is secreted out of the cell and can induce autoimmune phenotypes in mice. Elevated amounts of this isoform have been found in the serum of people with systemic lupus erythematosus²⁴. Recently, it has been shown that the splicing factors TIA-1 and PTB have antagonistic effects for the regulation of FAS alternative splicing: TIA-1 binds an intronic uridine-rich sequence to include exon 6, whereas PTB recognizes an exonic splicing silencer to promote exon 6 skipping²⁶.

Here we investigate how human SPF45 can influence alternative splicing. We show that SPF45 can induce exon 6 skipping in FAS premRNA. This activity depends on the UHM domain of SPF45, which binds ULMs in the splicing factors U2AF65, SF1 and SF3b155 in vitro. We determined the crystal structure of SPF45-UHM bound to a ULM peptide derived from the U2-snRNP component SF3b155 at 2.1-Å resolution. Structure-based mutational analysis shows that the alternative splicing regulation activity of SPF45 is dependent on UHM-ULM-type interactions, which presumably compete with UHMs in other splicing factors. The data demonstrate that interactions of SPF45 with the ULMs of constitutive splicing factors are involved in FAS exon 6 skipping and suggest a general role for UHM-ULM interactions in alternative splicing regulation.

RESULTS

SPF45 induces FAS exon 6 skipping with its UHM

SPF45 has previously been shown to influence 3' splice site recognition and to be required for alternative splicing autoregulation by Sxl³. Increased SPF45 expression has been detected in a variety of tumors²⁷. We used transient overexpression of SPF45 in HeLa cells to identify alternative splicing events affected by changes in the cellular concentration of this splicing factor (S.B. and J.V., unpublished data). One of the alternative splicing events identified affected *FAS* exon 6, which can be included or skipped to generate RNAs encoding pro- or antiapoptotic forms of the FAS receptor. SPF45 overexpression induced exon 6 skipping in a *FAS* minigene (**Fig. 2a**, compare lanes 1 and 2). The effect of SPF45 was specific, because overexpression of the protein did not lead to skipping of, for example, exon 6 of cyclin D–type binding protein-1 (GCIP) expressed through a minigene containing a comparable arrangement of exon and intron lengths (**Fig. 2b**).

To map the domain(s) important for this activity of SPF45, we repeated the same experiment with several mutants of SPF45. Deleting the N-terminal region had little effect on *FAS* alternative splicing, and the N-terminal region alone did not show any activity (**Fig. 2a**, compare lanes 3 and 5 to 2). Deletion of the G-patch reduced the splicing activity, and deletion of the UHM abolished it completely (**Fig. 2a**, lanes 6 and 7). The UHM domain alone, however, was capable of reproducibly inducing detectable levels of exon 6 skipping (**Fig. 2a**, lane 4). The expression of the SPF45 constructs was judged by western blot analysis (**Supplementary Fig. 1** online). The splicing experiments suggest that an intact UHM is necessary and sufficient for at least partial induction of *FAS* exon 6 skipping by SPF45.

Also consistent with the idea that SPF45 is relevant for FAS alternative splicing is the finding that reduction in the abundance of endogenous SPF45 by RNA interference (RNAi) resulted in increased levels of FAS exon 6 inclusion (**Fig. 2c**). In these experiments, to detect reliable differences in exon 6 inclusion, we used a FAS minigene

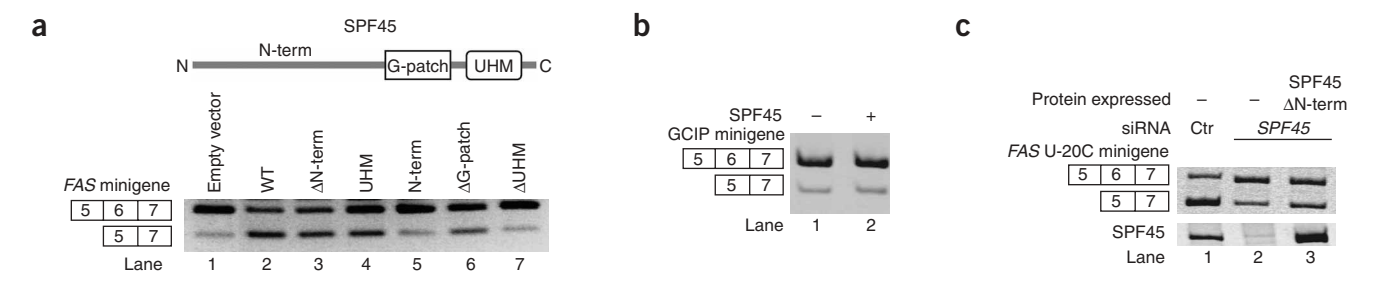


Figure 2 SPF45 induces exon 6 skipping in a *FAS* minigene. (a) Full-length or deletion-mutant SPF45 (as depicted in diagram) was overexpressed together with a *FAS* minigene comprising exons 5, 6 and 7. Splicing products were detected by RT-PCR analysis. For expression controls using western blotting, see **Supplementary Figure 1**. (b) As in **a**, but using a minigene encoding GCIP. (c) Analysis of alternative splicing of the *FAS* mutant U-20C minigene, showing effects of the depletion and rescue of SPF45. Abundance of *SPF45* mRNA was analyzed by RT-PCR (bottom gel). Ctr, control siRNA.

harboring a mutation at the polypyrimidine tract of intron 5 (U-20C) that increases exon 6 skipping²⁶. The effects of SPF45 depletion were at least partially reversed by overexpression of Δ N-term-SPF45, an active SPF45 deletion mutant (**Fig. 2a**) that lacks the sequences targeted by the siRNAs used to deplete the endogenous protein. Together, the results of **Figure 2** indicate that variations in the abundance of SPF45 influence *FAS* exon 6 inclusion and skipping.

SPF45-UHM binds motifs in U2AF65, SF1 and SF3b155

To understand the mechanism by which SPF45 induces exon skipping in FAS, we tested whether SPF45-UHM is capable of interacting with the conserved, tryptophan-containing ULM regions in U2AF65, SF1 and SF3b155. We used glutathione S-transferase (GST)-tagged ULM peptides of U2AF65 and SF1 in GST pull-down experiments and found that both ULMs tested bind SPF45-UHM (**Fig. 3a**, lanes 4 and 5). Isothermal titration calorimetry (ITC) yielded $K_{\rm d}$ values of 3.9 and 2.6 μ M for U2AF65₈₅₋₁₁₂ and SF1₁₋₂₅, respectively; these binding affinities are comparable to ULM interactions with other splicing factors (**Table 1** and **Supplementary Fig. 2** online).

Whereas U2AF65 and SF1 contain only one ULM each, the N terminus of SF3b155 contains five motifs that resemble the ULM consensus (**Fig. 1b**). It has previously been shown that U2AF65-UHM is capable of binding all five of these sites with low-micromolar

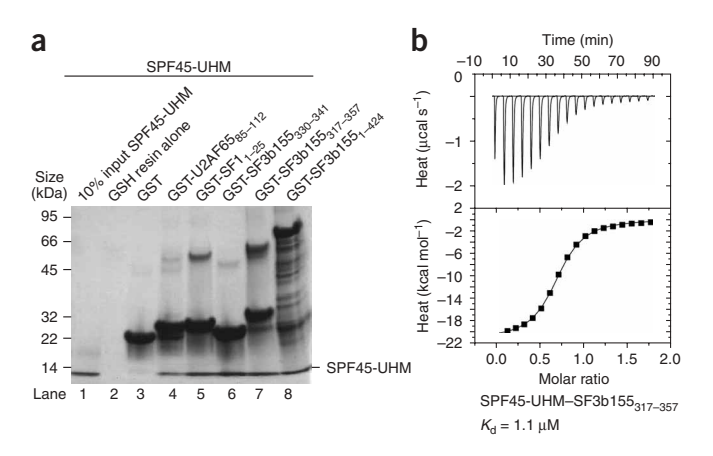


Figure 3 Analysis of SPF45-UHM–ULM interactions. (a) Coomassie-stained SDS-PAGE analysis of GST pull-down experiments. Indicated GST-tagged ULM peptides and controls were used to precipitate untagged SPF45-UHM with glutathione beads. (b) Isothermal calorimetry titration of SPF45-UHM and SF3b155-ULM5.

 $K_{\rm d}$ values, whereas it does not bind two additional regions with tryptophan residues that lack homology to ULMs^{18,19}. ULM1, ULM4 and ULM5 in SF3b155 are highly similar to the ULMs of SF1 and U2AF65, and comply with a strict consensus sequence, RKXRWDET, suggesting similar modes of binding to UHM domains. The region around SF3b155 Trp338 (in ULM5; Fig. 1b) is the most homologous to SF1. We found that a long and a shorter version (residues 317-357 and 333-342) of this ULM bind similarly to SPF45-UHM in GST pull-down experiments (Fig. 3a, lanes 6 and 7). Next, we compared binding of SPF45-UHM to SF3b155-ULM5 alone and to the whole N terminus (1-424) with GST pull-down experiments (Fig. 3a, lane 8) and ITC. SF3b155-ULM5 (317-357) bound with a K_d of 1.1 μM and a stoichiometry of 0.96 (Fig. 3b), whereas the full N terminus of SF3b155 (1–424) yielded an apparent K_d of 2.7 μ M and a stoichiometry of 2.3 (Supplementary Fig. 2). We conclude that SPF45-UHM recognizes at least two ULMs of SF3b155 but that the affinity for ULM5 is higher than the average affinity of all ULMs. In conclusion, these data show that SPF45 is able to bind several constitutive splicing factors through UHM-ULMtype interactions.

Structure of the SF3b155-ULM5-SPF45-UHM complex

To reveal molecular details of SPF45 UHM-ULM interactions, we crystallized SPF45-UHM in complex with SF3b155-ULM5 (residues 333–342) and determined the structure at 2.1-Å resolution.

As expected, SPF45-UHM adopts the characteristic $\beta\alpha\beta\beta\alpha\beta$ RRM fold (**Fig. 4a**). Residues 306–310 (β1), 337–343 (β2), 353–359 (β3) and 380–386 (β4) constitute an antiparallel β-sheet, which is covered by two helices, α A (321–333) and α B (362–369) on one side. In addition, SPF45-UHM residues 374–377 form a fifth strand, β3′, which extends the antiparallel β-sheet both in the free structure and in complex with SF3b155. A similar fifth strand has been described in the U1A–RNA²⁸ and U2AF35–U2AF65 (ref. 11) structures. SPF45-UHM also contains a C-terminal helix (α C, residues 389–394) and an extended C-terminal tail, which together occlude the potential RNA-binding site of the antiparallel β-sheet.

In the ULM-bound complex of SPF45-UHM, electron density is detectable for residues 334–342 of SF3b155. Seven of these residues (Ser336–Pro342) contact SPF45-UHM (**Fig. 4a,b**). The interaction with SF3b155 mainly involves the Arg-Xaa-Phe motif (formed by residues Arg375, Tyr376 and Phe377 and therefore called the Arg-Tyr-Phe motif below) of SPF45, which is located at the tip of the β -hairpin formed by strands $\beta 3'$ and $\beta 4$ (**Fig. 4a,b**). The side chain of Trp338 inserts into a hydrophobic pocket formed by helices αA and αB as well as hydrophobic side chains on the β -sheet (**Fig. 4b**). The



Table 1 Dissociation constants for UHM-ULM interactions determined by isothermal titration calorimetry

Dissociation constants (K _d)	SF1-ULM (1-25)	U2AF65-ULM (85-112)	SF3b155-ULM5 (317-357)
U2AF35-UHM (38-152)	$> 150~\mu M$	135 ± 9 nM	$> 150~\mu\text{M}$
U2AF65-UHM (377-475)	$1.6 \pm 0.04 \mu M$	$>$ 300 μ M	$6.7 \pm 0.2 \mu M$
SPF45-UHM (301-401)	$2.6 \pm 0.09 \; \mu M$	$3.9 \pm 0.2 \mu\text{M}$	$1.1 \pm 0.01 \mu M$

Shown are experimental values ± fitting error.

aromatic ring of SPF45 Phe377 forms an orthogonal interaction with SF3b155 Trp338 and stacks with the side chain of SF3b155 Arg337. This three-fold stacking interaction involving Phe377 of the Arg-Tyr-Phe motif and two ULM residues closely resembles the molecular recognition of SF1-ULM by U2AF65-UHM (**Fig. 4c**). Specificity is mediated by charged interactions: SF3b155 Arg337 forms electrostatic contacts with SPF45 Asp319 and Glu325, while SF3b155 Asp339 is coordinated by SPF45 Arg375. SPF45 Arg375 in turn is stabilized by a salt bridge with Glu329 on αA. The backbone amides and carbonyls of SF3b155-ULM5 (residues 337–340) form an extensive network of hydrogen bonds with backbone amides of the β-hairpin formed by strands β 3′ and β 4 (data not shown).

In the crystal, the basic N-terminal residues preceding the tryptophan in the SF3b155 peptide are involved in lattice formation and bind a symmetry-related SPF45 molecule (Supplementary Fig. 3 online). Nevertheless, we believe that in solution, electrostatic interactions between these residues and the negatively charged helix αA in SPF45 contribute to the binding. This is because in both the U2AF35-UHM–U2AF65-ULM and U2AF65-UHM–SF1-ULM complexes, specific salt bridges are not observed between the conserved basic ULM residues and acidic residues in helix αA of the UHM^{11,12}; yet mutations of positively charged residues in SF1 and negatively charged residues in helix αA of U2AF65-UHM have demonstrated the importance of long-range electrostatic contacts for this UHM-ULM interaction¹².

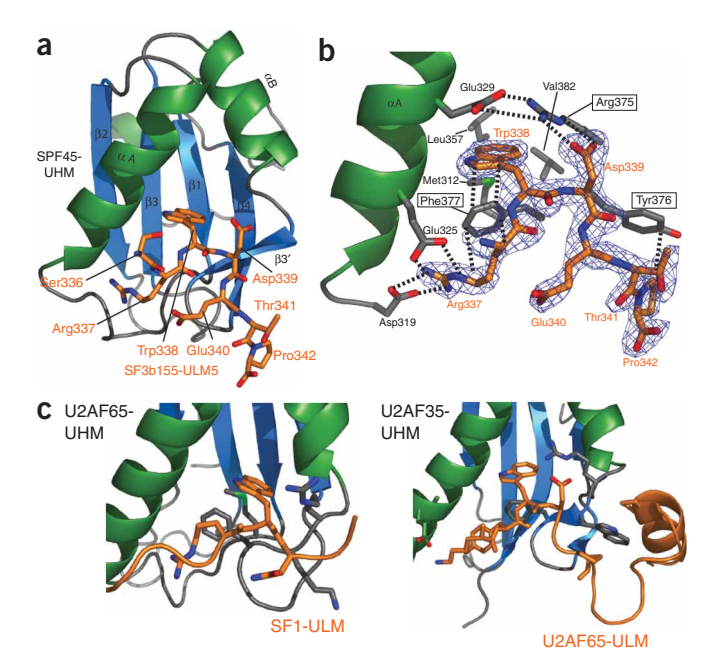
U2AF65, SF1 and SF3b155 ULM binding are similar

We next compared the binding of the ULM sequences of U2AF65, SF1 and SF3b155 to SPF45-UHM in NMR titration experiments. ULM peptides were added to ¹⁵N-labeled SPF45-UHM and the chemical shifts of the amide groups were monitored using ¹H, ¹⁵N NMR experiments. Addition of each of the tested ULM peptides induced substantial chemical shift perturbations (**Fig. 5a**). Whereas SF1 and SF3b155 induced strong and, for many signals, very similar chemical shift changes, the spectral changes induced by U2AF65 were different (**Fig. 5a**, close-up). This finding is consistent with the greater similarity of the SF1 and SF3b155 ULM sequences to each other than to the U2AF65 ULM (**Fig. 1b**). To locate the chemical shift perturbations induced by ULM binding, we assigned the backbone resonances of SPF45-UHM. The chemical shift perturbations observed

Figure 4 Crystal structure of SPF45-UHM bound to SF3b155-ULM5. (a) Ribbon representation of SPF45-UHM with stick representation of SF3b155-ULM5 peptide. (b) Details of the molecular recognition of SPF45-UHM and SF3b155-ULM5. Experimental omit-electron density map contoured at $1.8\ \sigma$ (blue) surrounds a stick representation of residues 337-342 of the SF3b155 peptide (orange). SPF45-UHM residues involved in ULM coordination are shown in gray. (c) Structures of the U2AF65-UHM-SF1-ULM complex (left, PDB 100P) and the U2AF35-UHM-U2AF65-ULM complex (right, PDB 1JMT).

in the titrations could then be mapped for all three ULM motifs onto the sequence of SPF45-UHM (**Fig. 5b**). Upon binding of SF1 and SF3b155 ULMs, two regions of SPF45-UHM are mainly affected. The first region comprises the loop following strand $\beta 1$ and parts of helix αA ; the second region extends from the end of helix αB and strand $\beta 3'$ (containing the Arg-Tyr-Phe motif) to strand $\beta 4.$ Overall, U2AF65-ULM induces weaker chemical shift perturbations than the other two ULMs, consistent with its weaker binding affinity (**Table 1**). Nevertheless, the strongest perturbations are located in the same regions as seen for SF1 and SF3b155. This shows that the molecular recognition of all three ULMs by SPF45 is similar.

The chemical shift perturbations affect almost all peaks in the NMR spectrum, which suggests some conformational changes of the UHM upon ULM binding. To locate these changes, we solved the crystal structure of the free SPF45 UHM at 2.0-Å resolution (Fig. 5c). The structures of free and SF3b155-ULM-bound SPF45 UHM superimpose with an r.m.s. deviation of 0.9 Å over 99 of 104 C α atoms. The largest structural changes occur in the loop between strand β1 and helix αA (Fig. 5c, left). NMR relaxation data (Supplementary Fig. 4a online) and B-factors of free and ligand-bound SPF45-UHM show that this loop is dynamic in the absence of the peptide and becomes ordered only when bound to the ULM. Furthermore, helix αA and strand $\beta 3'$ are shifted by ~ 5 Å toward each other upon binding of SF3b155-ULM5. This closing of the UHM is stabilized by the salt bridge between strand β3' (SPF45 Arg375) and helix αA (SPF45 Glu329). In contrast, in the free form, SPF45 Arg375 forms a salt bridge with Asp371. (Fig. 5c, left). None of the regions



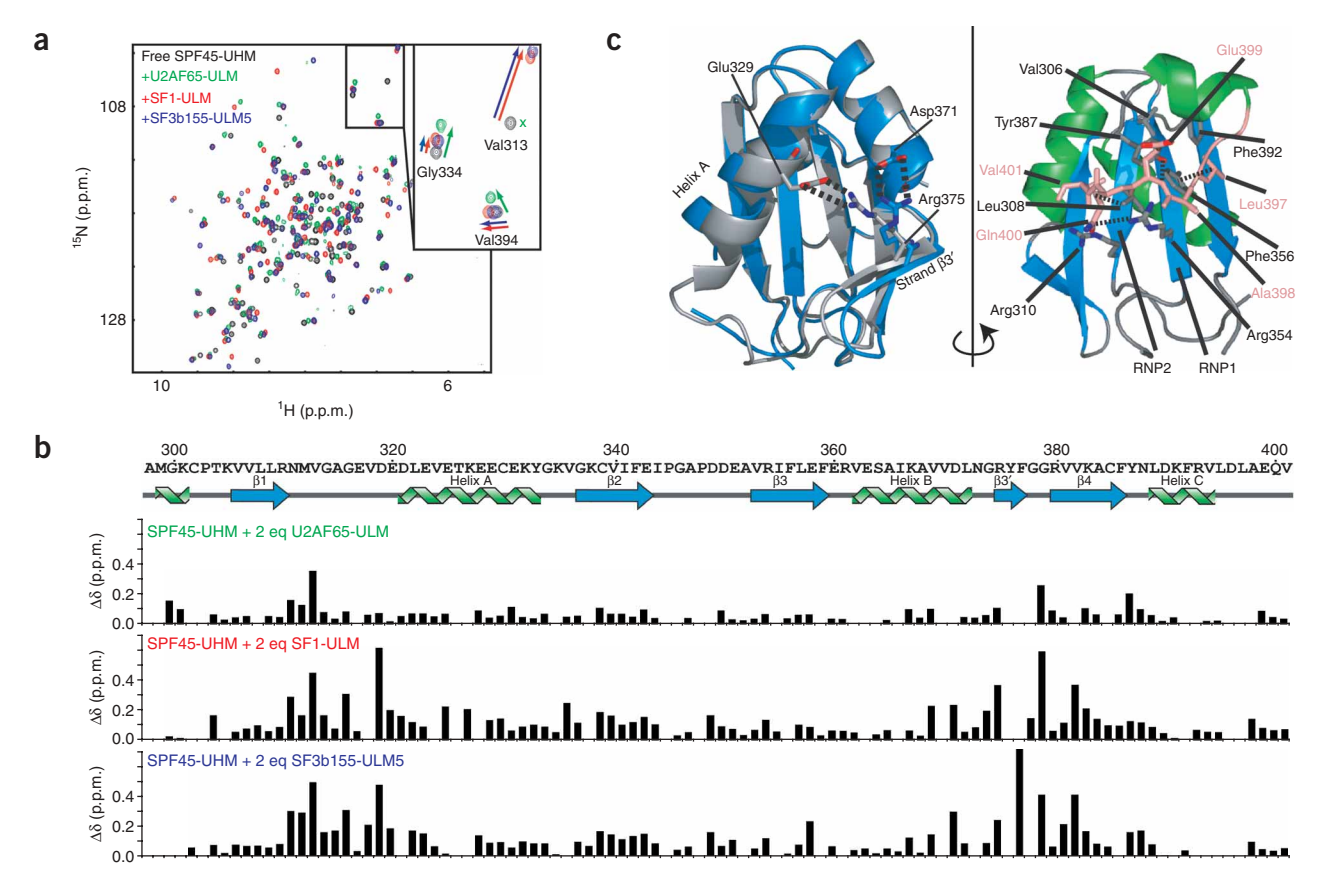


Figure 5 SPF45-UHM binds ULM peptides derived from U2AF65, SF1 and SF3b155. (a) Overlay of ^{1}H , ^{15}N correlation spectra of free 0.3 mM SPF45-UHM (black), upon addition of two-fold molar excess of U2AF65₈₅₋₁₁₂ (green), SF1₁₋₂₅ (red) or SF3b155₃₁₇₋₃₅₇ (blue). Colored arrows in the close-up view indicate directions of chemical shift perturbations. Green X indicates a peak broadened by intermediate exchange. (b) Chemical shift perturbations, $(\Delta\delta(^{1}\text{H})^{2}+(0.2\times\Delta\delta(^{15}\text{N}))^{2})^{1/2}$, upon binding of two molar equivalents of U2AF65-ULM (upper row), SF1-ULM (middle row) or SF3b155-ULM5 (lower row) are shown below the sequence of SPF45-UHM. Secondary structure representation at top is based on chemical shift-derived predictions using TALOS. (c) Left, comparison of crystal structures of free (blue) and SF3b155-ULM5-bound (gray) SPF45-UHM. Right, crystal structure of free SPF45, rotated by 180° compared with structures on the left.

in SPF45-UHM that change conformation upon binding SF3b155-ULM5 are involved in crystal-lattice formation.

SPF45-UHM and G-patch are unlikely to bind RNA

A previous study has found that Drosophila SPF45 can be sequencespecifically UV cross-linked to the upstream AG in the 3' splice site of Sxl exon 3 but not to a mutant pre-mRNA containing CG in the same position³. In addition, the *Toxoplasma gondii* ortholog of SPF45, TgDRE, has been shown to bind oligonucleotides with its G-patch⁷. Thus, if SPF45 binds RNA directly, this probably involves the G-patch, the UHM or both (see Fig. 1a). To test this, we titrated a heptamer RNA oligonucleotide derived from the β-thalassemic mutant β^{110} of the human β -globin gene (which has been shown to be a target of SPF45 activity³) into a human SPF45 construct comprising the G-patch and the UHM domains. No chemical shift perturbations were observable even at three-fold molar excess of RNA (Supplementary Fig. 4b), suggesting that neither the G-patch nor the UHM domains of SPF45 have appreciable RNA binding affinity. The poor chemical shift dispersion for the additional NMR signals, compared with Figure 5a, suggests that the G-patch is largely unstructured, and the lack of chemical shift perturbation upon RNA addition excludes the possibility that the G-patch becomes structured upon RNA binding.

In the SPF45 UHM structure, the β -sheet surface that is typically used to bind RNA in RRM–RNA complexes²⁸ is occluded by helix α C and the extended C terminus (**Fig. 5c**, right panel). NMR relaxation data show that the residues in the C-terminal extension are not flexible and presumably bind the β -sheet surface in solution as well (**Supplementary Fig. 4a**). Together, these data suggest that SPF45-UHM is unlikely to bind RNA (at least the oligonucleotide tested here) in a canonical manner independent of the absence or presence of a bound ULM. The previously reported cross-linking of SPF45 to the proximal 3' splice site of Sxl intron 2 (ref. 3) is most likely the result of SPF45 recruitment to a location near these sequences by other factors (see Discussion).

Splicing regulation requires UHM-ULM interactions

Next, we examined whether a UHM-ULM-type interaction could be involved in the exon-skipping activity of SPF45. For this, we designed mutations of SPF45-UHM that disrupt binding to the ULMs of U2AF65, SF1 and SF3b155. As two regions in SPF45-UHM coordinate the SF3b155 ULM (respectively comprising residues Asp319 and Glu325, and Arg375-Tyr376-Phe377; **Fig. 4b**), we tested the triple mutants D319A E320A D321A, D319K E320R D321K, R375A Y376A F377A, and R375D Y376A F377A.



Table 2 Summary of ULM binding and splicing activity of SPF45-UHM mutants

SPF45 mutations	U2AF6	5-ULM	SF1-	ULM	SF3b15	5-ULM5	HeLa assay
Triple	Prediction	Pull-down	Prediction	Pull-down	Prediction	Pull-down	
D319A E320A D321A	?	_	No	_	No	_	_
D319K E320R D321K	?	_	No	_	No	_	_
R375A Y376A F377A	No	(+)	No	(+)	No	-	_
R375D Y376A F377A	No	-	No	-	No	-	-
Selective							
F377A	?	(+)	?	(+)	No	-	_
F377Y	?	+++	?	(+)	?	++	_
Y376A	No	-	?	(+)	No	-	_
R375A	No	-	Yes	(+)	No	-	_
E329Q	?	-	?	++	?	(+)	(+)
D319A	Yes	++	No	-	No	(+)	-
Nonselective							
D319K	?	-	No	-	No	-	ND
E320K	Yes	++	Yes	++	Yes	++	++
E320A	Yes	++	Yes	++	Yes	++	ND
D321A	Yes	++	Yes	++	Yes	++	ND
D319K D321K	?	_	No	_	No	_	ND
R375D	No	-	?	-	No	=-	ND

For each ULM, table lists predicted interactions and the results of GST pull-down experiments: 'No' denotes no binding predicted; 'Yes', binding predicted; question mark, prediction not clear; +++, binding stronger than wild-type SPF45 in pull-down assay; ++, binding close to wild-type; (+), reduced binding compared with wild-type; -, no detectable binding. Last column shows outcomes of splicing assays using a FAS minigene and the indicated full-length SPF45 mutant in HeLa cells: - denotes no increase in exon 6 skipping; (+), slight increase in exon 6 skipping similar to wild-type SPF45; ND, splicing activity not determined.

One-dimensional NMR spectra confirmed that the tertiary folding of the mutant proteins is not altered (data not shown). GST pull-down experiments showed that the mutants have no or strongly reduced binding affinity for the U2AF65, SF1 and SF3b155 ULM peptides (**Table 2** and **Fig. 6a**). None of the triple mutations induces *FAS* exon 6 skipping *in vivo* (**Table 2** and **Fig. 6b**). As these mutations are designed to specifically disrupt SPF45-UHM interactions with ULM-type ligands, we conclude that the splice site–switching activity of SPF45 requires binding of its UHM to one or more ULM-type ligands *in vivo*.

Mutations can selectively disrupt ULM interactions

The finding that SPF45's effect on FAS alternative splicing involves UHM-ULM-type interactions prompts the question of which of the ULM-containing proteins could be a ligand of SPF45 relevant for its activity in vivo. To address this, we exploited the sequence differences between the ULMs (Fig. 6c) to design structure-based selective mutations of SPF45-UHM that disrupt binding to a subset of ULMs, but not all ULMs. From analysis of the complex structure (Fig. 4), several residues of SPF45-UHM can be predicted to be differentially involved in binding SF3b155, SF1 and U2AF65 (Table 2 and Fig. 6c; for a detailed rationale, see Supplementary Methods online). The results of GST pull-down binding assays with SPF45 harboring alanine and/or charge-reversal mutations of Asp319, Glu320, Glu329, Arg375, Tyr376 and Phe377 (the latter three comprising the Arg-Tyr-Phe motif) are summarized in Table 2 and shown in Figure 6d. These experiments show that although F377A binds with somewhat lower affinity to U2AF65-ULM, the mutation has appreciably stronger effects on binding to SF1-ULM and SF3b155-ULM5, thus providing some quantitative discrimination between ULMs. Several other mutations with discriminatory potential were found. For example, F377Y binds even more strongly than wild-type SPF45 to U2AF65-ULM, weakly to SF1-ULM and almost

like wild-type SPF45 to SF3b155-ULM5. Y376A and R375A bind to SF1-ULM with weaker than wild-type affinity and not at all to U2AF65-ULM and SF3b155-ULM5. E329Q binds SF1-ULM with somewhat lower than wild-type affinity but shows a much stronger effect on binding to SF3b155-ULM5 and, particularly, on binding to U2AF65-ULM. In contrast, D319A binds to U2AF65-ULM with close to wild-type affinity but very weakly to SF1-ULM and with reduced affinity to SF3b155-ULM5. D319K does not bind any of the ULMs, whereas E320K binds all three ULMs. This was expected, as Glu320 is not involved in coordinating SF3b155-ULM5 in the crystal structure, even though it is next to Asp319, which, in contrast, mediates crucial interactions for peptide binding.

We also tested binding with the full N terminus of SF3b155 (1–424), which contains five potential ULMs. The full SF3b155 N terminus has binding selectivity for the SPF45-UHM mutants that is very similar to that of ULM5 alone (317–357) (**Supplementary Fig. 5c** online). This may be explained by the sequence similarities of the ULM sequences in SF3b155. Three of them contain the consensus RWDETP, which is the main interaction region in the crystal structure. The other two are less conserved and probably have a lower affinity for SPF45-UHM, consistent with the apparent stoichiometry of 2.3 derived by ITC.

ULM-selective mutants are functionally inactive

Finally, we expressed the ULM-selective SPF45 mutants together with the FAS minigene in HeLa cells to test whether the mutations affected alternative splicing differentially. None of the mutants that show binding selectivity in GST pull-down assays (F377A, F377Y, Y376A, R375A and D319A; **Fig. 6d**) has any detectable splicing-regulation activity in HeLa cells (**Fig. 6e**). Only the mutant E329Q has a weak activity in inducing skipping of exon 6 when cotransfected with the FAS minigene. As a control, we used the mutant E320K, which binds

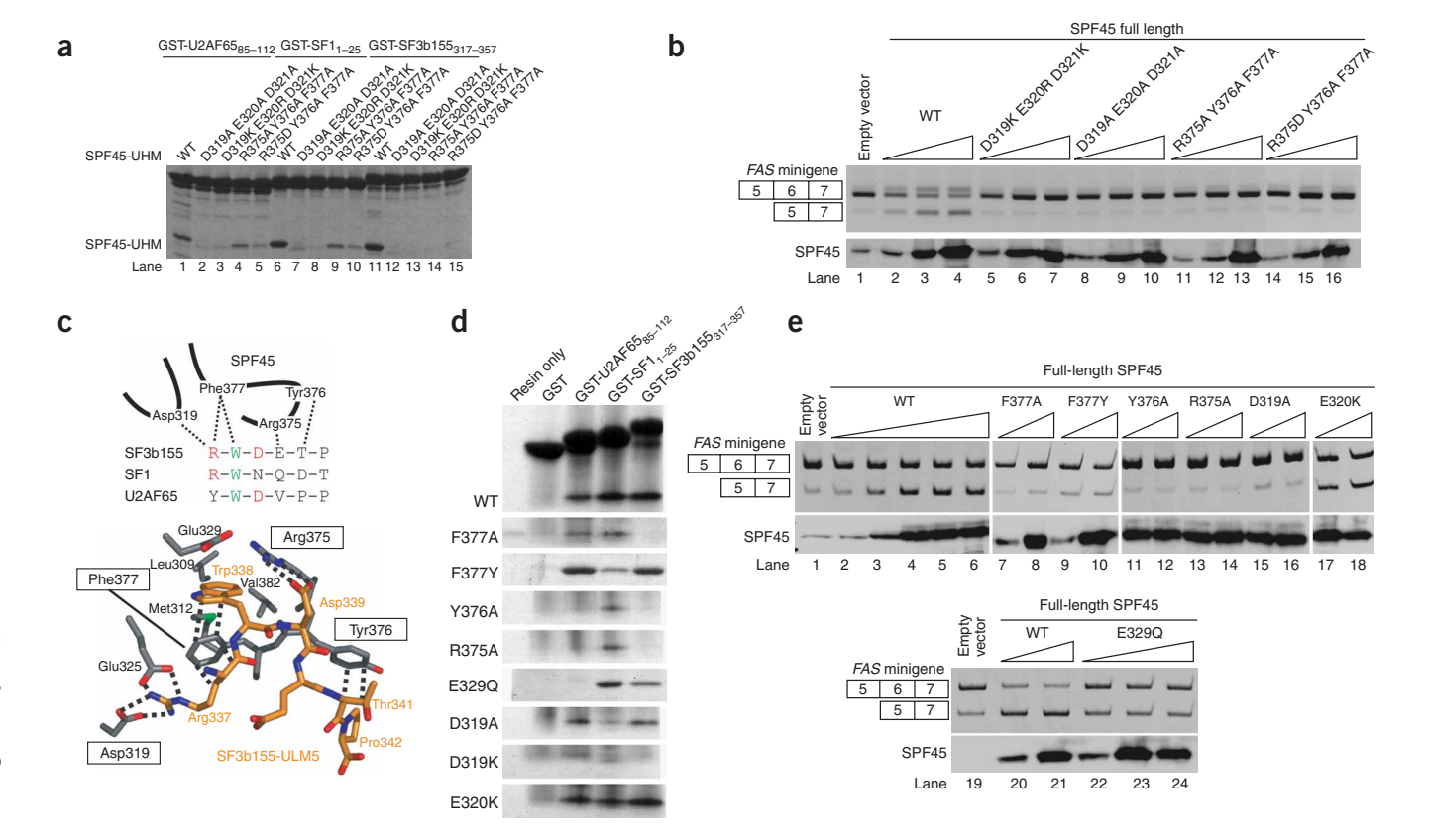


Figure 6 GST pull-down binding experiments and *FAS* splicing assays using SPF45-UHM mutants. (a) Coomassie-stained SDS-PAGE analysis of GST pull-down experiments. GST-tagged U2AF65-ULM, SF1-ULM and SF3b155-ULM5 were used to precipitate untagged wild-type (WT) or mutant SPF45-UHM with glutathione beads. For input controls, glutathione beads alone and GST-controls, see **Supplementary Figure 5a**. (b) RT-PCR analysis of expression of *FAS* isoforms (top) and western blots with SPF45-specific antibodies as expression control (bottom), after coexpression of *FAS* and WT or mutant SPF45 in HeLa cells. (c) Top, schematic drawing of important interactions between SPF45-UHM and SF3b155-ULM5 found in the crystal structure. Sequences of SF1 and U2AF65 ULMs are shown for comparison. Bottom, details of molecular recognition of SPF45-UHM (gray) and SF3b155-ULM5 (orange) from the crystal structures. (d) Coomassie-stained SDS-PAGE analyses of GST pull-down experiments. The indicated GST-tagged ULM peptides were used to precipitate WT or mutant SPF45-UHM with glutathione beads. See **Supplementary Figure 5b** for the full gel images. (e) *FAS* splicing assay in HeLa cells, as in b, with the full-length SPF45-UHM mutants used in d.

all three ULMs like wild-type SPF45, as mentioned above. Accordingly, E320K has the same activity as wild-type SPF45 in the HeLa splicing assay. The levels of expression of the different mutants were comparable to those of the wild-type protein (**Fig. 6e**, lower gels). Together, the structural and functional data strongly support the idea that UHM-mediated interactions are essential for SPF45-mediated regulation of alternative splicing.

DISCUSSION

Our data show that UHM-ULM-type protein-protein interactions are important for the regulation of alternative splicing by SPF45. The results summarized in **Figure 6** suggest that the interaction of SPF45-UHM with SF1-ULM is crucial for the activity of SPF45: none of the SPF45 mutants for which this interaction is substantially compromised is active in splicing regulation, whereas mutant E329Q, which shows only slightly reduced binding to SF1-ULM, has substantial residual splicing regulation activity. The lower than wild-type activity of the E329Q mutant may reflect either the lower binding affinity between the SPF45-UHM and SF1-ULM or the reduced binding between SPF45-UHM and SF3b155-ULM observed in the GST pull-down experiments (**Fig. 6d**). This indicates that binding to SF1, or binding to SF1 and strong binding to SF3b155, is necessary for *FAS*

splicing regulation by SPF45. The function of SPF45 could involve the (sequential) binding and release of ULMs in these factors. Thereby, ULM interactions of SPF45-UHM may compete with UHM-ULM interactions of constitutive splicing factors required for exon 6 inclusion. For example, SPF45-UHM could replace the interactions of U2AF65-UHM with SF1-ULM or SF3b-ULM. A sequential binding model requires a regulated release of certain UHM-ULM interactions and subsequent contacts between other UHM-ULM pairs. ULM release could, for example, be induced by phosphorylation, as has been shown for SF1 (ref. 29). The SF3b155 N terminus is also phosphorylated and dephosphorylated during splicing^{30–32}. However, in preliminary experiments, we could not observe an effect of phosphorylation of SF3b155-ULM5 on the binding affinity for SPF45-UHM (data not shown). Nevertheless, sequential formation and release of multiple UHM-ULM interactions remains a possible explanation for splicing regulation by SPF45, according to our data.

The residual splicing-regulation activity of the E329Q mutant, which does not bind U2AF65-ULM, suggests that a putative interaction between SPF45-UHM and U2AF65-ULM is dispensable for FAS alternative splicing in HeLa cells. This is consistent with the fact that U2AF65-ULM binds much more tightly to U2AF35-UHM^{11,15,33}

than to SPF45-UHM, so that a displacement of U2AF35-UHM by SPF45-UHM seems unlikely.

A further possible explanation for the behavior of our mutants would be that SPF45 must bind a ULM different from those of U2AF65, SF1 and SF3b155 tested in this study. In fact, ULM-like sequences can be found in many proteins, owing to the shortness and degeneracy of the established ULMs. A forward screen would be necessary to identify additional potential ligands of SPF45.

Our data imply that, in humans, splicing regulation by SPF45 depends on its interactions with constitutive splicing factors. In regard to this, it is noteworthy that recruitment of SPF45 to a regulated 3' splice site region in the *Drosophila Sxl* gene depends on the polypyrimidine tract and the 3' splice site AG (ref. 3), which are recognized by the 65- and 35-kDa subunits of U2AF, respectively. This suggests that the SPF45-UHM-ULM interactions reported here could facilitate SPF45 association with this RNA. In fact, we found that a region comprising the G-patch and the UHM domain of SPF45 cannot bind an AG-containing RNA ligand on its own. Thus, the previously reported sequence-specific cross-linking of SPF45 to a splice-site AG unusually located upstream of the polypyrimidine tract in Sxl exon 3 (ref. 3) probably depends on other factors. For example, an interaction of SPF45-UHM with SF1-ULM or SF3b155-ULM, or both, could help in recruiting SPF45 to the AG dinucleotide. Thus, UHM-ULM interactions similar to those described here for FAS splicing regulation could also have a role in the regulation of alternative splicing of Drosophila Sxl.

Our data suggest an interesting link between alternative splicing by SPF45 and the regulation of apoptosis by FAS in cancer cells. *In vivo*, SPF45 overexpression is observed in many cancers, such as breast, colon, lung and ovarian tumors²⁷. We found that overexpression of SPF45 in HeLa cells, a cervical carcinoma cell line, leads to *FAS* exon 6 skipping. The finding that, in addition to TIA-1 and PTB²⁶, SPF45 is involved as well in the alternative splicing regulation of *FAS* exon 6 suggests that the switch in expression between pro- and anti-apoptotic FAS isoforms is tightly controlled. In fact, the amount of apoptosis must be carefully balanced *in vivo* to ensure the functionality of the immune system and to prevent the death of intact cells at the same time²⁵. We speculate that SPF45 overexpression might be a means for tumor cells to escape apoptosis.

In summary, our data imply a role for the splicing factor SPF45 in apoptosis regulation through FAS/CD95 that depends on its UHM. The network of UHM-ULM-type interactions might have a more widespread function in the regulation of additional alternative splicing events. Given that about 75% of human transcripts have alternative isoforms³⁴, more transcripts may be found that can be alternatively spliced through the action of SPF45. Finally, SPF45 seems to use diverse molecular mechanisms to modulate alternative splicing of different substrates, showing that the regulation of alternative splicing is multifaceted and involves multiple pathways that allow for tight control.

METHODS

Protein preparation. Recombinant U2AF65-UHM (residues 369–475), U2AF35-UHM (38–152), SPF45-UHM (301–401) SPF45–G-patch–UHM (234-401), PUF60–UHM (457–556), HCC1-UHM (418–511) and KIS-UHM (320–411) were expressed from modified pET9d vectors (pETM30, http://www.embl.de/ExternalInfo/protein_unit/draft_frames/) with tobacco etch virus (TEV)–cleavable N-terminal His₆-thioredoxin tags. SF3b155₁₄₂₄, SF3b155_{317–357}, SF3b155_{330–341}, U2AF65_{85–112} and SF1_{1–25} were expressed from pETM30 vectors with TEV-cleavable His₆-GST tags. Unlabeled proteins were expressed in *Escherichia coli* BL21(DE3) in LB medium. Isotopically ¹⁵N- and

 $^{13}\text{C}\text{-labeled}$ proteins were expressed in minimal (M9) medium supplemented with $^{15}\text{NH}_4\text{Cl}$ or $^{15}\text{NH}_4\text{Cl}$ and $^{13}\text{C}\text{-D}\text{-glucose}.$ All proteins were purified with nickel–nitrilotriacetic acid agarose (Qiagen) under standard conditions. Constructs used for crystallography or NMR were further purified on a Superdex-75 (Pharmacia) gel-filtration column. NMR samples were concentrated to 0.7-1.0 mM in 20 mM Na₂HPO₄ buffer (pH 6.8) with 150 mM NaCl and 5 mM β -mercaptoethanol. Synthetic SF3b155₃₃₃₋₃₄₂ peptide was purchased from Peptide Specialty Laboratory, Heidelberg, and used without further purification.

Crystallization and data collection. For crystallization, SPF45-UHM in 20 mM Tris (pH 7.0) and 150 mM NaCl at 24 mg ml $^{-1}$ was mixed in 1:2.5 ratio with the SF3B155 $_{333-342}$ peptide. Crystals of the complex were grown at room temperature by vapor diffusion in sitting drops composed of equal volumes (100 nl each) of protein solution and crystallization buffer (25% (w/v) PEG 1,500, 0.1 M malonate-imidazole-borate (MIB, molar ratios 2:3:3) buffer (pH 6.0)). They grew to a size of about 150 µm × 150 µm × 100 µm and were cryoprotected by serial transfer into reservoir solution containing 20% (v/v) glycerol. Cryogenic data at 2.1-Å resolution were recorded using a rotating anode source equipped with osmic mirrors (Rigaku) and a MAR345 image plate detector(MAR Research). Crystals of free SPF45-UHM grew in 22% (w/v) PEG 3,350, 0.2 M MgCl₂ and 0.1 M Tris (pH 8.5). The crystals were frozen directly in the cryostream, and a complete data set at 2.0-Å resolution was recorded at beamline ID14-1 of the European Synchrotron Radiation Facility. See **Table 3** for data collection details.

Structure determination and refinement. The structure of free SPF45-UHM was solved by molecular replacement as implemented in PHASER³⁵. The search model was generated with the program MODELLER³⁶ using the structure of U2AF65-UHM (PDP 100P)¹². The solution comprises one SPF45 monomer in the asymmetric unit and was refined in alternating cycles of model correction using COOT³⁷ and restrained TLS refinement as implemented in REFMAC5³⁸.

Table 3 Data collection and refinement statistics

	SPF45 (free form)	SPF45 (SF3b155 complex)		
Data collection				
Space group	F222	P 2 ₁ 2 ₁ 2 ₁		
Cell dimensions				
a, b, c (Å)	63.9, 90.2, 99.1	45.9, 66.4, 72.7		
α , β , γ (°)	90.0, 90.0, 90.0	90.0, 90.0, 90.0		
Resolution (Å)	19.58-2.00 (2.05-2.00)	38.84-2.11 (2.114-2.110)		
R_{sym}^{a}	0.053	0.045		
$I / \sigma I^a$	20.13 (4.67)	32.56 (9.46)		
Completeness (%) ^a	99.5 (100.0)	89.3 (78.5)		
Redundancy ^a	7.57 (7.2)	7.1 (6.75)		
Refinement				
Resolution (Å)	19.58-2.00	38.84-2.11		
No. reflections	9,294	13,008		
R _{work} / R _{free} ^b	0.231 / 0.244	0.208 / 0.272		
No. atoms				
SPF45	1,538	3,241		
SF3b peptide	-	303		
Water	30	93		
B-factors				
Protein	58.1	26.1		
Ligand/ion	-	28.0		
Water	54.6	26.7		
R.m.s. deviations				
Bond lengths (Å)	0.010	0.013		
Bond angles (°)	1.236	1.385		

Values in parentheses are for highest-resolution shell. $^{\rm a}$ As defined in XDS $^{\rm 46}.$ $^{\rm b}$ As defined in REFMAC5.

In the final model, 92.9%, 7.1%, 0% and 0% of residues are in the most favored, favored, generously allowed and disallowed regions of the Ramachandran plot, respectively. The structure of SPF45 in complex with SF3b155_{333–342} was determined with PHASER using the refined model of free SPF45-UHM. The solution comprises two molecules in the asymmetric unit and shows clear difference density for the two peptide moieties. Structural quality was checked with PROCHECK³⁹. Structural visualization was done with PyMOL (http://pymol.sourceforge.net/). In the final model, 90.8%, 8.7%, 0.5% and 0% of residues are in the most favored, favored, generously allowed and disallowed regions of the Ramachandran plot, respectively. See Table 3 for structure statistics.

NMR experiments. NMR spectra were recorded at 303 K on Bruker DRX500 and DRX600 spectrometers, processed with NMRPipe40 and analyzed with NMRView⁴¹. Backbone ¹H, ¹⁵N and ¹³C resonances of free SPF45-UHM were assigned with standard triple-resonance experiments⁴². φ/ψ torsion-angle restraints were derived with TALOS⁴³. For NMR titrations, chemical shifts were measured with ¹H, ¹⁵N HSQC experiments. ¹⁵N relaxation data were recorded at 500-MHz ¹H frequency as described⁴⁴ using a 2-kHz spin-lock field for the ¹⁵N T_{1p} experiments. The RNA used for the NMR titration was purchased from Biospring and is derived from a 3' splice site in the β-thalassemic mutation of the human β-globin gene³.

Isothermal titration calorimetry. Binding affinities of UHM domains for ULM ligands were measured using an MCS isothermal titration calorimeter (MicroCal). Before calorimetry, both interaction partners were dialyzed against 50 mM sodium phosphate buffer (pH 7.0), 150 mM NaCl and 2 mM β-mercaptoethanol. ULM concentrations were adjusted to 400 μM, UHM concentrations to 30– $40 \,\mu\text{M}$. The ULM was injected into 1.4 ml UHM solution in steps of 15 µl. Data were processed with the manufacturer's software, MicroCal Origin 5.0. Errors were evaluated by Levenberg-Marquardt nonlinear fits.

Glutathione S-transferase pull-down experiments. GST-tagged ULMs (30 μg) were mixed with 30 μg (\sim 3 equivalents) of untagged UHMs in 100 μl PBS buffer supplemented with 2 mM β-mercaptoethanol and 0.1% (v/v) IGEPAL at 4 °C and mixed vigorously for 1 h. For GST precipitation, 3 μg of glutathione-Sepharose (GSH; 4B, Amersham) was added and mixed vigorously for 15 min. The glutathione-Sepharose was sedimented by centrifugation and washed twice with the buffer described above. Results were analyzed on Coomassie- or silverstained SDS-PAGE gels.

Splicing assays in HeLa cells. Exponentially grown HeLa cells were transfected at 50% confluency ($\sim 5 \times 10^6$ cells) with either 0.25 µg of FAS reporter plasmid DNA corresponding to genomic sequences between exons 5 and 7 (ref. 43) or 0.25 µg of GCIP reporter plasmid DNA corresponding to genomic sequences from exon 5 to 30 nucleotides into intron 7, and with 1–2 μg of an expression vector where a full-length or deletion-mutant version of the SPF45 open reading frame sequence was cloned between a cytomegalovirus (CMV) promoter and polyadenylation signals using Exgen 500 (Fermentas). Cells were then incubated for 24 h before cytoplasmic RNA was isolated (RNeasy, Qiagen) and analyzed by reverse-transcription PCR (RT-PCR) and electrophoresis as described $^{26,45}\!.$ SPF45 expression was evaluated by western blotting using 20 μg of total cellular protein and antibodies raised in rabbits against full-length SPF45 expressed in E. coli. The mutant constructs used correspond to the following changes in the SPF45 protein: ΔN-Term, deletion of amino acid residues 8-230; UHM, residues 1-7 fused to residues 300-401; N-term, truncation to residues 1–230; ΔG-patch, deletion of residues 231–299; ΔUHM, deletion of residues 300-395.

RNA interference. Cells were transfected at 30% confluency ($\sim 3 \times 10^6$ cells) with either a control RNA or three different short interfering RNAs (siRNAs) targeting SPF45 mRNA, using Lipofectamine 2000 (Invitrogen) according to the manufacturer's recommendations. After 48 h, the U-20C minigene was transfected with or without ΔN -term SPF45–encoding plasmid. The cells were collected 24 h later and the experiment conducted as described above. Depletion of SPF45 mRNA was analyzed by RT-PCR using the following primers: Fwd, 5'-CTAAGTGTCCTACTAAAGTGGT-3'; Rev, 5'-TCAAAC

TTGTTCTGCCAAATCCAA-3'. Several independent experiments were carried out, with consistent results. siRNA sequences (Stealth siRNA from Invitrogen) were as follows: SPF45_1, 5'-GCUCCUCAGAUGACCGGCAAAUUGU-3'; SPF45_2, 5'-UAGCUGACGAAUAUGACCCUAUGUU-3'; SPF45_3, 5'-AAGG AGACCAGAUCCAGAUUCUGAU-3'; Ctr_siRNA, 5'-AAGAGCCGAUACC GAUACUUAGGAU-3'.

Accession codes. Protein Data Bank: Coordinates and structure factors have been deposited with accession codes 2PE8 (free SPF45-UHM) and 2PEH (SF3b155-ULM5-bound SPF45-UHM).

Note: Supplementary information is available on the Nature Structural & Molecular Biology website.

ACKNOWLEDGMENTS

We thank the staff at the European Synchrotron Radiation Facility and Swiss Light Source for assistance during data collection, V. Rybin (European Molecular Biology Laboratory, EMBL) for ITC measurements, I. Sinning and I. Tews (University of Heidelberg) for ITC measurement time, G. Stier (EMBL) for expression vectors, and B. Simon (EMBL) for help with NMR measurements. M.H. is a fellow of the Peter and Traudl Engelhorn Foundation. This work was supported by the Deutsche Forschungsgemeinschaft (Sa 823/5) and EU grant 3D Repertoire (LSHG-CT-2005-512028).

AUTHOR CONTRIBUTIONS

L.C. performed biochemistry, NMR experiments and data analysis; L.C. and J.B. performed crystallization and crystallographic data collection; L.C. and M.H. interpreted the crystallographic data; S.B. carried out molecular biology splicing activity assays; K.S. provided resources; M.S., J.V., L.C. and S.B. conceived the study and wrote the paper.

COMPETING INTERESTS STATEMENT

The authors declare no competing financial interests.

Published online at http://www.nature.com/nsmb/ Reprints and permissions information is available online at http://npg.nature.com/ reprintsandpermissions

- 1. Black, D.L. Mechanisms of alternative pre-messenger RNA splicing. Annu. Rev. Biochem. 72, 291-336 (2003).
- Bell, L.R., Horabin, J.I., Schedl, P. & Cline, T.W. Positive autoregulation of sex-lethal by alternative splicing maintains the female determined state in Drosophila. Cell 65, 229-239 (1991).
- 3. Lallena, M.J., Chalmers, K.J., Llamazares, S., Lamond, A.I. & Valcarcel, J. Splicing regulation at the second catalytic step by Sex-lethal involves 3' splice site recognition by SPF45. Cell 109, 285-296 (2002).
- Aravind, L. & Koonin, E.V. G-patch: a new conserved domain in eukarvotic RNAprocessing proteins and type D retroviral polyproteins. Trends Biochem. Sci. 24, 342-344 (1999).
- Silverman, E.J. et al. Interaction between a G-patch protein and a spliceosomal DEXD/ H-box ATPase that is critical for splicing. Mol. Cell. Biol. 24, 10101-10110 (2004).
- Svec, M., Bauerova, H., Pichova, I., Konvalinka, J. & Strisovsky, K. Proteinases of betaretroviruses bind single-stranded nucleic acids through a novel interaction module, the G-patch. FEBS Lett. 576, 271-276 (2004).
- Frenal, K. et al. Structural and functional characterization of the TgDRE multidomain protein, a DNA repair enzyme from *Toxoplasma gondii. Biochemistry* 45, 4867–4874
- Chaouki, A.S. & Salz, H.K. Drosophila SPF45: a bifunctional protein with roles in both splicing and DNA repair. PLoS Genet. 2, e178 (2006).
- Kielkopf, C.L., Lucke, S. & Green, M.R. U2AF homology motifs: protein recognition in the RRM world. Genes Dev. 18, 1513-1526 (2004).
- 10. Maris, C., Dominguez, C. & Allain, F.H. The RNA recognition motif, a plastic RNAbinding platform to regulate post-transcriptional gene expression. FEBS J. 272, 2118-2131 (2005).
- 11. Kielkopf, C.L., Rodionova, N.A., Green, M.R. & Burley, S.K. A novel peptide recognition mode revealed by the X-ray structure of a core U2AF35/U2AF65 heterodimer. Cell 106, 595-605 (2001).
- 12. Selenko, P. et al. Structural basis for the molecular recognition between human splicing factors U2AF65 and SF1/mBBP. Mol. Cell 11, 965-976 (2003).
- 13. Berglund, J.A., Abovich, N. & Rosbash, M. A cooperative interaction between U2AF65 and mBBP/SF1 facilitates branchpoint region recognition. Genes Dev. 12, 858-867 (1998).
- 14. Rain, J.C., Rafi, Z., Rhani, Z., Legrain, P. & Krämer, A. Conservation of functional domains involved in RNA binding and protein- protein interactions in human and Saccharomyces cerevisiae pre-mRNA splicing factor SF1. RNA 4, 551-565 (1998).
- 15. Rudner, D.Z., Kanaar, R., Breger, K.S. & Rio, D.C. Interaction between subunits of heterodimeric splicing factor U2AF is essential in vivo. Mol. Cell. Biol. 18, 1765-1773 (1998).



- Gozani, O., Potashkin, J. & Reed, R. A potential role for U2AF-SAP 155 interactions in recruiting U2 snRNP to the branch site. Mol. Cell. Biol. 18, 4752–4760 (1998).
- Das, R., Zhou, Z. & Reed, R. Functional association of U2 snRNP with the ATP-independent spliceosomal complex E. Mol. Cell 5, 779–787 (2000).
- Thickman, K.R., Swenson, M.C., Kabogo, J.M., Gryczynski, Z. & Kielkopf, C.L. Multiple U2AF65 binding sites within SF3b155: thermodynamic and spectroscopic characterization of protein-protein interactions among pre-mRNA splicing factors. *J. Mol. Biol.* 356, 664–683 (2006).
- Spadaccini, R. et al. Biochemical and NMR analyses of an SF3b155-p14–U2AF-RNA interaction network involved in branch point definition during pre-mRNA splicing. RNA 12, 410–425 (2006).
- Page-McCaw, P.S., Amonlirdviman, K. & Sharp, P.A. PUF60: a novel U2AF65-related splicing activity. RNA 5, 1548–1560 (1999).
- 21. Van Buskirk, C. & Schupbach, T. Half pint regulates alternative splice site selection in *Drosophila. Dev. Cell* **2**, 343–353 (2002).
- Jung, D.J., Na, S.Y., Na, D.S. & Lee, J.W. Molecular cloning and characterization of CAPER, a novel coactivator of activating protein-1 and estrogen receptors. *J. Biol. Chem.* 277, 1229–1234 (2002).
- Dowhan, D.H. et al. Steroid hormone receptor coactivation and alternative RNA splicing by U2AF65-related proteins CAPERalpha and CAPERbeta. Mol. Cell 17, 429–439 (2005).
- 24. Cheng, J. *et al.* Protection from Fas-mediated apoptosis by a soluble form of the Fas molecule. *Science* **263**, 1759–1762 (1994).
- Krammer, P.H. CD95's deadly mission in the immune system. Nature 407, 789–795 (2000).
- Izquierdo, J.M. et al. Regulation of Fas alternative splicing by antagonistic effects of TIA-1 and PTB on exon definition. Mol. Cell 19, 475–484 (2005).
- Sampath, J. et al. Human SPF45, a splicing factor, has limited expression in normal tissues, is overexpressed in many tumors, and can confer a multidrug-resistant phenotype to cells. Am. J. Pathol. 163, 1781–1790 (2003).
- Allain, F.H. et al. Specificity of ribonucleoprotein interaction determined by RNA folding during complex formulation. Nature 380, 646–650 (1996).
- Wang, X. et al. Phosphorylation of splicing factor SF1 on Ser20 by cGMP-dependent protein kinase regulates spliceosome assembly. EMBO J. 18, 4549–4559 (1999).
- Boudrez, A., Beullens, M., Waelkens, E., Stalmans, W. & Bollen, M. Phosphorylation-dependent interaction between the splicing factors SAP155 and NIPP1. *J. Biol. Chem.* 277, 31834–31841 (2002).
- Wang, C. et al. Phosphorylation of spliceosomal protein SAP 155 coupled with splicing catalysis. Genes Dev. 12, 1409–1414 (1998).

- Shi, Y., Reddy, B. & Manley, J.L. PP1/PP2A phosphatases are required for the second step of Pre-mRNA splicing and target specific snRNP proteins. *Mol. Cell* 23, 819–829 (2006).
- Zhang, M., Zamore, P.D., Carmo-Fonseca, M., Lamond, A.I. & Green, M.R. Cloning and intracellular localization of the U2 small nuclear ribonucleoprotein auxiliary factor small subunit. *Proc. Natl. Acad. Sci. USA* 89, 8769–8773 (1992).
- 34. Johnson, J.M. *et al.* Genome-wide survey of human alternative pre-mRNA splicing with exon junction microarrays. *Science* **302**, 2141–2144 (2003).
- McCoy, A.J., Grosse-Kunstleve, R.W, Storoni, L.C. & Rean, R.J. Likelihood-enhanced fast translation functions. *Acta Crystallogr. D Biol. Crystallogr.* 61, 458–464 (2005).
- Sali, A. & Blundell, T.L. Comparative protein modelling by satisfaction of spatial restraints. J. Mol. Biol. 234, 779–815 (1993).
- Emsley, P. & Cowtan, K. Coot: model-building tools for molecular graphics. Acta Crystallogr. D Biol. Crystallogr. 60, 2126–2132 (2004).
- Murshudov, G.N., Vagin, A.A. & Dodson, E.J. Refinement of macromolecular structures by the maximum-likelihood method. *Acta Crystallogr. D Biol. Crystallogr.* 53, 240–255 (1997)
- Laskowski, R.A., MacArthur, M.W., Moss, D.S. & Thornton, J.M. PROCHECK: a program to check the stereochemical quality of protein structures. *J. Appl. Cryst.* 26, 283–291 (1993).
- Delaglio, F. et al. NMRPipe: a multidimensional spectral processing system based on UNIX pipes. J. Biomol. NMR 6, 277–293 (1995).
- 41. Johnson, B.A. & Blevins, R.A. NMRView: a computer program for the visualization and analysis of NMR data. *J. Biomol. NMR* **4**, 603–614 (1994).
- Sattler, M., Schleucher, J. & Griesinger, C. Heteronuclear multidimensional NMR experiments for the structure determination of proteins in solution employing pulsed field gradients. *Prog. Nucl. Magn. Reson. Spectrosc.* 34, 93–158 (1999).
- Cornilescu, G., Delaglio, F. & Bax, A. Protein backbone angle restraints from searching a database for chemical shift and sequence homology. *J. Biomol. NMR* 13, 289–302 (1999).
- Korzhnev, D.M., Skrynnikov, N.R., Millet, O., Torchia, D.A. & Kay, L.E. An NMR experiment for the accurate measurement of heteronuclear spin-lock relaxation rates. *J. Am. Chem. Soc.* 124, 10743–10753 (2002).
- Forch, P. et al. The apoptosis-promoting factor TIA-1 is a regulator of alternative premRNA splicing. Mol. Cell 6, 1089–1098 (2000).
- Kabsch, W. Automatic processing of rotation diffraction data from crystals of initially unknown symmetry and cell constants. J. Appl. Cryst. 26, 795–800 (1993).



Erratum: U2AF-homology motif interactions are required for alternative splicing regulation by SPF45

Lorenzo Corsini, Sophie Bonnal, Jerome Basquin, Michael Hothorn, Klaus Scheffzek, Juan Valcárcel & Michael Sattler *Nat. Struct. Mol. Biol.* 14, 620–629 (2007); published online 24 June 2007; corrected after print 2 July 2007

In the version of this article initially published, the name of the second author, Sophie Bonnal, was misspelled. The error has been corrected in the HTML and PDF versions of the article. We apologize for this error.

